

## COMBINATION PARAMETRIC AND INTERNAL RESONANCES OF AN AXIALLY MOVING BEAM

**Bamadev Sahoo<sup>1</sup>, L. N. Panda<sup>2</sup>, G. Pohit<sup>\*3</sup>**

<sup>1</sup> Department of Mechanical Engineering, International Institute of Information Technology,  
Bhubaneswar, India  
bamdev\_sahoo@yahoo.com

<sup>2</sup> College of Engineering and Technology, Bhubaneswar. <sup>3</sup> Department of Mechanical Engineering,  
Jadavpur University, Kolkata, India

<sup>2</sup>lnpanda@yahoo.com, <sup>3</sup>gpohit@gmail.com

**Keywords:** Bifurcation, Chaos, Stability, Perturbation technique, Combination parametric resonance.

**Abstract.** *This paper deals with nonlinear planar vibration of a travelling beam subjected to combination parametric resonance in the presence of internal resonance. The beam is simply supported at both ends and the travelling velocity is assumed to be comprised of a harmonically varying component superimposed over a mean velocity. The geometric cubic nonlinearity in the equation of motion is due to stretching effect of the beam. The natural frequency of second mode is approximately three times the natural frequency of first mode for a range of mean velocity of the beam, resulting in a three-to-one internal resonance. The analysis is done using the method of multiple scales (MMS) by directly attacking the governing nonlinear integral-partial-differential equations and the associated boundary conditions. The resulting set of first-order ordinary differential equations governing the modulation of amplitude and phase of the first two modes is analyzed numerically. The stability, bifurcation and response behavior of the beam is investigated for combination parametric resonance in presence of internal resonance. The system exhibits trivial and two mode closed loop and isolated solutions with saddle-node and Hopf bifurcations. The dynamic response of the system is illustrated by periodic, mixed mode, quasiperiodic and chaotic behavior in terms of two dimensional phase portraits, Poincare maps, time traces and FFT power spectra. This wide array of dynamic response of the system shows the influence of internal resonance.*

## 1 INTRODUCTION

Axially moving beams are present in a wide range of engineering applications, such as serpentine belts, aerial cables, magnetic tapes, power transmission belts, band saw blades. Real-life axially moving systems rarely travel at a constant axial speed even when they are designed to be. The vast literature on axially moving continua vibration has been reviewed by Wickert and Mote [1] up to 1988. Wickert and Mote [2, 3] studied the transverse vibration of axially moving strings and beams using an eigen function method. Oz et.al [4, 5] investigated principal and combination parametric resonances and stability analysis for an axially accelerating beam using the method of multiple scales. Riedel and Tan [6] studied the coupled and forced behavior of an axially moving strip with internal resonance. Ozkaya et al [7] investigated non-linear transverse vibrations and 3:1 internal resonances of a beam with multiple supports and plotted frequency response curves for different support numbers. Chin et.al [8] and Panda et.al [9, 10] investigated the principal parametric resonance and combination parametric resonance of hinged-clamped beams and pipe conveying pulsating fluid respectively. Ding et.al [11] used Galerkin methods for finding natural frequencies of high-speed axially moving beams with hybrid boundary conditions. Pakdemirli *et. al* [12] studied the transverse vibration of simply supported axially moving Euler-Bernoulli beam for infinite mode analysis and truncation to resonant modes. Ponomareva *et. al* [13] investigated transversal vibrations of axially travelling continua based on a string model at the low frequencies and a tensioned beam model at the higher frequencies. Recently a systematic research on travelling beam was pursued by Ghayesh et.al [14, 15] involving non-linear dynamic phenomenon of a variety of system models.

The present investigation is combination parametric resonance of first two modes in which the influence of internal resonance is demonstrated by the two mode equilibrium solutions of both amplitude and frequency response analysis. Besides the two mode solutions there is trivial mode solution. The system exhibits Hopf and saddle node bifurcations for different control parameters. The dynamic behavior of the system is illustrated in terms of periodic, mixed mode, quasiperiodic and chaotic responses.

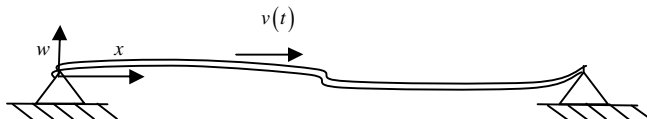


Figure 1: Schematic diagram of an axially traveling simply supported beam with variable velocity.

## 2 FORMULATION OF THE PROBLEM

Figure 1 shows a uniform horizontal beam simply supported at both ends and travelling with a harmonically variable velocity. The beam is assumed to be an Euler-Bernoulli beam in transverse vibration and nonlinearity is geometric in nature due to the mid-plane stretching effect of the beam. The non-dimensional equation of transverse motion of the beam considering viscous damping [16] and viscoelastic damping [17] is given by

$$\ddot{w} + 2\nu\dot{w}' + \dot{\nu}w' + (v^2 - 1)w'' + v_f^2 w'''' + 2\varepsilon\alpha\dot{w}'''' + 2\varepsilon\mu\dot{w} = \frac{1}{2}v_t^2 w'' \int_0^1 w'^2 dx \quad (1)$$

The non dimensional scheme used here is

$$x = \frac{x^*}{L}, t = t^* \sqrt{\frac{P}{\rho A L^2}}, w = \frac{w^*}{L}, v = \frac{v^*}{\sqrt{P/\rho A}}, 2\varepsilon\alpha = \frac{E^*}{L^2} \left( \frac{I}{mE} \right)^{1/2}$$

$$2\varepsilon\mu = \frac{CL^2}{\sqrt{mEI}}, v_l = \sqrt{\frac{EA}{P}}, v_f = \sqrt{\frac{EI}{PL^2}}$$

where the variables with asterisk denote dimensional ones, dot denotes derivatives with respect to time and prime denotes derivatives with respect to spatial derivative  $x$ .  $m$  is mass per unit length,  $\rho$  is density,  $A$  is cross sectional area,  $L$  is length,  $v_f$  is non dimensional flexural stiffness and  $v_l$  nondimensional longitudinal stiffness of beam.  $E^*$  the coefficient of internal dissipation of the beam material (Kelvin-Voigt type).  $C$  is the external damping factor,  $\alpha$  is nondimensional material damping and  $\mu$  is nondimensional viscous damping. Reordering the transverse displacement with the relation  $w = \sqrt{\varepsilon} w^\#$ , where  $\varepsilon < 1$ , the system is converted into a weakly nonlinear one [5] which may be represented as (removing superscript “#”)

$$\ddot{w} + 2v\dot{w}' + v\dot{w}' + (v^2 - 1)w'' + v_f^2 w'''' + 2\varepsilon\alpha \dot{w}'''' + 2\varepsilon\mu \dot{w} = \frac{1}{2} \varepsilon v_l^2 w'' \int_0^1 w'^2 dx \quad (2)$$

The variable velocity of the beam is  $v = v_0 + \varepsilon v_1 \sin \Omega t$  (3) where  $v_0$  is mean velocity,  $\varepsilon v_1$  is amplitude and  $\Omega$  is the frequency of the harmonically varying component. From equation (3) in (2), one gets the equation of transverse motion

$$2\varepsilon\alpha \dot{w}'''' + v_f^2 w'''' + [v_0^2 + 2\varepsilon v_0 v_1 \sin \Omega t - 1] w'' + \varepsilon v_1 \Omega w' \cos \Omega t + 2(v_0 + \varepsilon v_1 \sin \Omega t) \dot{w}' + 2\varepsilon\mu \dot{w} + \ddot{w} = \frac{1}{2} \varepsilon v_l^2 w'' \int_0^1 w'^2 dx \quad (4)$$

$$\text{with boundary conditions} \quad w(0, t) = w(1, t) = w''(0, t) = w''(1, t) = 0 \quad (5)$$

### 3 METHOD OF ANALYSIS

An approximate solution to this weakly non-linear distributed parameter system in the form of a first order uniform expansion by using the direct perturbation technique of method of multiple scales (MMS) [8-10] is aimed. The time scale used here is  $T_n = \varepsilon^n t$ ,  $n = 0, 1, 2, 3 \dots$  and the time derivatives are

$$\frac{d}{dt} = D_0 + \varepsilon D_1 + \dots, \quad \frac{d^2}{dt^2} = D_0^2 + 2\varepsilon D_0 D_1 + \dots, \quad D_n = \frac{\partial}{\partial T_n}, \quad n = 0, 1, 2, 3, \dots \quad (6)$$

$$\text{Assuming an expansion of the form } w(x, t, \varepsilon) = w_0(x, T_0, T_1) + \varepsilon w_1(x, T_0, T_1) + \dots \quad (7)$$

and equating coefficients of like powers of  $\varepsilon$  on both sides, we get

$$O(\varepsilon^0): D_0^2 w_0 + 2v_0 D_0 w_0' + (v_0^2 - 1)w_0'' + v_f^2 w_0'''' = 0$$

$$w_0(0, t) = w_0(1, t) = w_0''(0, t) = w_0''(1, t) = 0 \quad (8)$$

$$\begin{aligned}
 O(\varepsilon^1): D_0^2 w_1 + 2v_0 D_0 w_1' + v_f^2 w_1'' + (v_0^2 - 1) w_1'' = -2v_0 D_1 w_0' - 2v_1 \sin \Omega t D_0 w_0' - 2D_0 D_1 w_0 \\
 - 2\alpha D_0 w_0'' - 2\mu D_0 w_0 - 2v_0 v_1 \sin \Omega t w_0'' - v_1 \Omega \cos \Omega t w_0' + \frac{1}{2} v_1^2 w_0'' \int_0^1 w_0'^2 dx = 0 \quad (9) \\
 w_1(0, t) = w_1(1, t) = w_1''(0, t) = w_1''(1, t) = 0
 \end{aligned}$$

The solution of equation (8) may be written as

$$w_0(T_0, T_1, x) = \sum_{n=1}^{\infty} \phi_n(x) A_n(T_1) e^{i\omega_n T_0} + cc \quad (10)$$

where  $\phi_n$  are the mode shapes,  $\omega_n$  are the natural frequencies, and  $cc$  is complex conjugate. The mode shapes are calculated previously [4]

$$\begin{aligned}
 \phi_n(x) = C_{1n} \left\{ e^{i\beta_{1n}x} - \frac{(\beta_{4n}^2 - \beta_{1n}^2)(e^{i\beta_{3n}} - e^{i\beta_{1n}})}{(\beta_{4n}^2 - \beta_{2n}^2)(e^{i\beta_{3n}} - e^{i\beta_{2n}})} e^{i\beta_{2n}x} - \frac{(\beta_{4n}^2 - \beta_{1n}^2)(e^{i\beta_{2n}} - e^{i\beta_{1n}})}{(\beta_{4n}^2 - \beta_{3n}^2)(e^{i\beta_{2n}} - e^{i\beta_{3n}})} e^{i\beta_{3n}x} \right. \\
 \left. + \left[ -1 + \frac{(\beta_{4n}^2 - \beta_{1n}^2)(e^{i\beta_{3n}} - e^{i\beta_{1n}})}{(\beta_{4n}^2 - \beta_{2n}^2)(e^{i\beta_{3n}} - e^{i\beta_{2n}})} + \frac{(\beta_{4n}^2 - \beta_{1n}^2)(e^{i\beta_{2n}} - e^{i\beta_{1n}})}{(\beta_{4n}^2 - \beta_{3n}^2)(e^{i\beta_{2n}} - e^{i\beta_{3n}})} \right] e^{i\beta_{4n}x} \right\} \quad (11)
 \end{aligned}$$

where  $\beta_{in}$  are eigen values which satisfy the dispersive relation Eq.(12) and support condition Eq.(13) [4]

$$v_f^2 \beta_{in}^4 - (v_0^2 - 1) \beta_{in}^2 - 2v_0 \omega_n \beta_{in} - \omega_n^2 = 0, \quad i = 1, 2, 3, 4 \quad (12)$$

$$\begin{aligned}
 (e^{i(\beta_{1n} + \beta_{2n})} + e^{i(\beta_{3n} + \beta_{4n})})(\beta_{1n}^2 - \beta_{2n}^2)(\beta_{3n}^2 - \beta_{4n}^2) + (e^{i(\beta_{1n} + \beta_{3n})} + e^{i(\beta_{2n} + \beta_{4n})})(\beta_{2n}^2 - \beta_{4n}^2) \\
 (\beta_{3n}^2 - \beta_{1n}^2) + (e^{i(\beta_{2n} + \beta_{3n})} + e^{i(\beta_{1n} + \beta_{4n})})(\beta_{1n}^2 - \beta_{4n}^2)(\beta_{2n}^2 - \beta_{3n}^2) = 0 \quad (13)
 \end{aligned}$$

Since the higher modes will decay with time due to the presence of damping and coriolis terms present in the equation, the first two modes will contribute to the long term system response. Consequently, Eq. (10) is replaced by

$$w_0(T_0, T_1, x) = A_1(T_1) \phi_1(x) e^{i\omega_1 T_0} + A_2(T_1) \phi_2(x) e^{i\omega_2 T_0} + cc \quad (14)$$

The frequency relations for the internal and combination parametric resonances are

$$\omega_2 = 3\omega_1 + \varepsilon\sigma_1 \quad \text{and} \quad \Omega = \omega_1 + \omega_2 + \varepsilon\sigma_2 \quad (15)$$

where  $\sigma_1$  and  $\sigma_2$  are detuning parameters. Substituting Eqs (14) and (15), into Eq.(9), we get

$$\begin{aligned}
 D_0^2 w_1 + 2v_0 D_0 w_1' + (v_0^2 - 1) w_1'' + v_f^2 w_1'' = \Gamma_1 e^{i\omega_1 T_0} + \Gamma_2 e^{i(\omega_1 T_0 + \sigma_1 T_1)} + \Gamma_3 e^{i\omega_2 T_0} + \Gamma_5 e^{i\omega_2 T_0} \\
 + \Gamma_6 e^{i(\omega_2 T_0 - \sigma_1 T_1)} + \Gamma_8 e^{i\omega_1 T_0} + cc + NST \quad (16)
 \end{aligned}$$

where the terms  $\Gamma_n$  are defined in the Appendix.  $NST$  do not produce secular or small divisor terms. As the homogeneous part of Eq.(16) with its associated boundary conditions has a nontrivial solution, the corresponding non homogeneous problem has a solution only if a solvability condition is satisfied. This requires the right hand side of Eq. (16) to be orthogonal to every solution of the adjoint homogeneous problem, which leads to the complex variable modulation equations for amplitude and phase

$$2A_1' + 8S_1A_1^2\bar{A}_1 + 8S_2A_1A_2\bar{A}_2 + 8g_1\bar{A}_1^2A_2e^{i\sigma_1T_1} + 2\mu C_1A_1 + 2\alpha e_1A_1 + 2K_4\bar{A}_2e^{i\sigma_2T_1} = 0 \quad (17)$$

$$2A_2' + 8S_4A_2^2\bar{A}_2 + 8S_3A_1A_2\bar{A}_1 + 8g_2A_1^3e^{-i\sigma_1T_1} + 2\mu C_2A_2 + 2\alpha e_2A_2 + 2K_5\bar{A}_1e^{i\sigma_2T_1} = 0 \quad (18)$$

where the prime denotes the differentiation with respect to slow time  $T_1$  and  $S_i, g_i, k_i, C_i$  and  $e_i$  are defined in the Appendix. Over bar indicates complex conjugate. The terms in the above equations involving the internal frequency detuning parameter  $\sigma_1$  are the contributions of the internal resonance in the system.

### 3 STABILITY AND BIFURCATION

The evolutions of the equilibrium solutions, their stability and bifurcation analysis for combination parametric resonance are carried out from the modulation Eqs. (17-18). Using

$$A_n = \frac{1}{2} [p_n(T_1) - i q_n(T_1)] e^{i\lambda_n(T_1)}, n = 1, 2 \quad (19)$$

The modulation equations are obtained as

$$\begin{aligned} p_1' = & -\mathfrak{G}_1 q_1 - S_{1R} (p_1^3 + p_1 q_1^2) - S_{1I} (p_1^2 q_1 + q_1^3) - S_{2R} (p_1 p_2^2 + p_1 q_2^2) - S_{2I} (q_1 p_2^2 + q_1 q_2^2) \\ & - g_{1R} (p_1^2 p_2 - p_2 q_1^2 + 2p_1 q_1 q_2) + g_{1I} (2p_1 q_1 p_2 - p_1^2 q_2 + q_1^2 q_2) - \mu C_{1R} p_1 \\ & - \mu C_{1I} q_1 - \alpha e_{1R} p_1 - \alpha e_{1I} q_1 - K_{4R} p_2 + K_{4I} q_2 \end{aligned} \quad (20)$$

$$\begin{aligned} q_1' = & \mathfrak{G}_1 p_1 + S_{1I} (p_1^3 + p_1 q_1^2) - S_{1R} (p_1^2 q_1 + q_1^3) - S_{2R} (q_1 p_2^2 + q_1 q_2^2) + S_{2I} (p_1 p_2^2 + p_1 q_2^2) \\ & + g_{1R} (2p_1 q_1 p_2 - p_1^2 q_2 + q_1^2 q_2) + g_{1I} (2p_1 q_1 q_2 + p_1^2 p_2 - p_2 q_1^2) - \mu C_{1R} q_1 + \mu C_{1I} p_1 \\ & - \alpha e_{1R} q_1 + \alpha e_{1I} p_1 + K_{4I} p_2 + K_{4R} q_2 \end{aligned} \quad (21)$$

$$\begin{aligned} p_2' = & -\mathfrak{G}_2 q_2 - S_{4R} (p_2^3 + p_2 q_2^2) - S_{4I} (q_2^3 + p_2^2 q_2) - S_{3R} (p_1^2 p_2 + p_2 q_1^2) - S_{3I} (p_1^2 q_2 + q_1^2 q_2) \\ & - g_{2R} (p_1^3 - 3p_1 q_1^2) + g_{2I} (q_1^3 - 3p_1^2 q_1) - \mu C_{2R} p_2 - \mu C_{2I} q_2 \\ & - \alpha e_{2R} p_2 - \alpha e_{2I} q_2 - K_{5R} p_1 + K_{5I} q_1 \end{aligned} \quad (22)$$

$$\begin{aligned} q_2' = & \mathfrak{G}_2 p_2 - S_{4I} (q_2^3 + p_2^2 q_2) + S_{4R} (p_2^3 + p_2 q_2^2) - S_{3R} (p_1^2 q_2 + q_1^2 q_2) + S_{3I} (p_1^2 p_2 + p_2 q_1^2) \\ & + g_{2R} (q_1^3 - 3p_1^2 q_1) + g_{2I} (p_1^3 - 3p_1 q_1^2) - \mu C_{2R} q_2 + \mu C_{2I} p_2 \\ & - \alpha e_{2R} q_2 + \alpha e_{2I} p_2 + K_{5I} p_1 + K_{5R} q_1 \end{aligned} \quad (23)$$

$$\text{Where } \mathfrak{G}_1 = \frac{1}{4}(\sigma_1 + \sigma_2) \text{ and } \mathfrak{G}_2 = \frac{1}{4}(3\sigma_2 - \sigma_1) \quad (24)$$

Above equations are perturbed to evaluate the stability. The perturbed equation is

$$\{\Delta p_1' \ \Delta q_1' \ \Delta p_2' \ \Delta q_2'\}^T = [J_c] \{\Delta p_1 \ \Delta q_1 \ \Delta p_2 \ \Delta q_2\}^T \quad (25)$$

where  $T$  denotes transpose and  $[J_c]$  is the Jacobian matrix whose eigen values determine the stability and bifurcation of the system. The stability boundary for trivial state is obtained by setting  $p_1 = q_1 = p_2 = q_2 = 0$ . The nonlinear steady state response behavior of the system is obtained from the normalized reduced Eqs. (20-23) by setting  $p_1' = q_1' = p_2' = q_2' = 0$ . The analysis for dynamic solutions is carried out by numerically integrating the Eqs. (20-23) with different combinations of system parameters.

## 4 RESULT AND DISCUSSIONS

The natural frequencies of the beam are numerically evaluated at different mean velocities ( $v_0$ ) with flexural stiffness  $\nu_f = 0.2$  by simultaneous solution of dispersive relation (Eq. (12)) and support condition (Eq. (13)). For a value of  $\nu_f = 0.2$ , it is noticed that at non dimensional mean velocity is  $v_0 = 0.513$  and the natural frequency of second mode is approximately

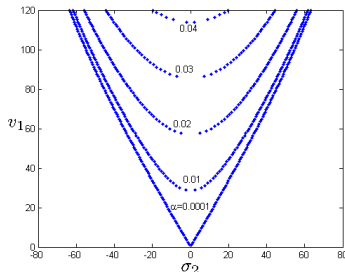


Figure 2: Trivial state boundary for different values of damping parameter.

equal to three times that of the first mode indicating the existence of 3:1 internal resonance. It is also noticed that, there are no other commensurable frequency relationships involving higher modes, so nonlinear interaction among higher modes is ruled out. The case of combination parametric resonance ( $\Omega \approx \omega_1 + \omega_2$ ) in presence of internal resonance in the subcritical mean velocity regime of a travelling beam is analyzed. The trivial state stability boundary shown in Figure 2 is plotted in terms of principal parametric frequency detuning ( $\sigma_2$ ) and amplitude of fluctuating velocity component ( $v_1$ ) for system parameters  $\nu_f = 0.2, v_1 = 40, v_0 = 0.7, \omega_1 = 2.7388, \omega_2 = 9.1403$  and for different material damping values. The book keeping parameter is taken as  $\varepsilon = 0.01$  and the corresponding internal frequency detuning parameter is assumed to be  $\sigma_1 = 92.39$ . The region inside the boundary denotes instability.

### 4.1 Stability and bifurcations of equilibrium solutions

Stability and bifurcation of the equilibrium solutions at each point are obtained from the eigenvalues of the Jacobean matrix of Eqs. (20-23). The continuation algorithm used in the analysis is cross checked by plotting the frequency response and amplitude response curves of Chin *et. al* [8] and the results are found to be in good agreement (not shown here). Figure 3 shows typical frequency response curves for first and second mode. Unlike principal parametric resonance of first and second modes, it doesn't have the single mode solution. It is observed that the closed loop curves are confined between two limit points  $SN_1(\sigma_2 = 22.5021)$  and  $SN_2(\sigma_2 = 128.982)$ . The upper stable branch of the closed loop loses stability through Hopf bifurcation. With further increase in the external frequency detuning parameter ( $\sigma_2$ ) along the same path, the system gains stability via reverse Hopf bifurcation at  $H_4(\sigma_2 = 84.246)$  and the stability of the system continues until a saddle node bifurcation occurs at point  $SN_2(\sigma_2 = 128.982)$  where the system response jumps to either the trivial stable or the nontrivial unstable equilibrium branch depending on the initial conditions. The other nontrivial solution branch has the limit point at  $SN_3(\sigma_2 = 125.350)$ , where the system jumps to one of two stable equilibrium solutions, one trivial and another nontrivial closed loop solu-

tion, depending on the initial conditions. With increase in  $\sigma_2$ , the amplitude of second mode ( $a_2$ ) increases monotonically up to a fixed value for stable branch of closed loop nontrivial equilibrium solution while for first mode, it increases first then decreases. The influence of internal detuning parameter ( $\sigma_1$ ) on frequency response for first and second mode is shown in Figure 4. The strength of nonlinear interaction due to 3:1 internal resonance gets weakened and amplitudes of both modes decrease when  $\sigma_1$  decreases from 92.39(Figure 3) to 44.00 (Figure 4).

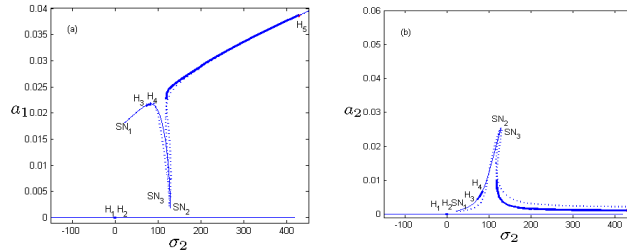


Figure 3: Frequency response curves for the first and second modes when a combination parametric resonance of the additive type is excited for system parameters  $\mu = 0.1$ ,  $\alpha=0$ ,  $\nu_1 = 10$ ,  $\nu_l = 40$  and  $\sigma_1 = 92.39$ .

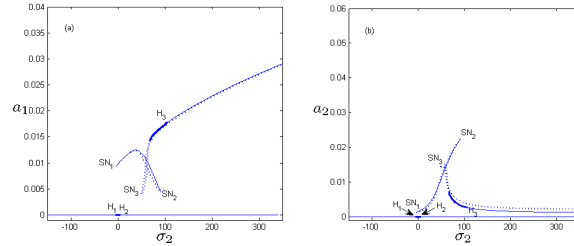


Figure 4: Frequency response curves for the first and second modes when a combination parametric resonance of the additive type is excited for system parameters  $\mu = 0.1$ ,  $\alpha=0$ ,  $\nu_1 = 10$ ,  $\nu_l = 40$  and  $\sigma_1 = 44.00$ .

## 5.2. Dynamic solutions

Dynamic response of the system is investigated in the vicinity of the frequency response curves. The results for particular system parameters are shown in Figures 4 (a, b). They are found to be dependent on initial conditions. Figures 5(a-d) show typical system response ( $\sigma_2 = 41.2201$ ) corresponding to the stable branch of isolated closed loop two mode solution of the frequency response curve (Figure 4). When the time integration is started with the initial values of  $p_1 = 0.0102$ ,  $q_1 = 0.0071$ ,  $p_2 = 0.0037$  and  $q_2 = 0.0070$ , the system response for both modes jumps from trivial state to nontrivial periodic solution as has been captured by the phase portraits (a, b) and time traces (c, d) in Figure 5. Figures 6 (a-d) show modulated mixed mode response period-8 for first mode and period-6 for second mode as illustrated by the time traces at  $\sigma_2 = 74.5201$  on the same curve. At another point on the curve, typically  $\sigma_2 = 82.5201$ , the system response becomes quasiperiodic as illustrated by the closed loop Poincare maps for both modes in Figures 7(a, b). For a wide range of  $\sigma_2$  system response remains quasiperiodic. Figures 8 (a-d) capture how the response changes to chaotic motion through quasiperiodic route for both modes.

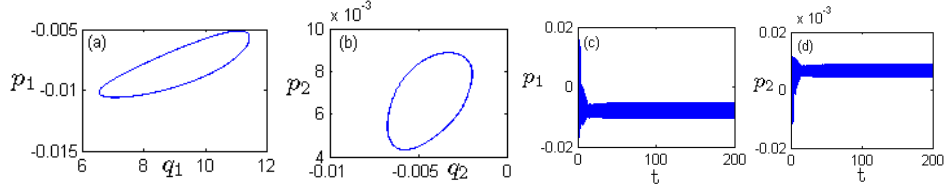


Figure 5: Phase portraits (a, b) and time traces(c, d) in the stable branch of isolated closed loop two mode solution of the frequency response curve (Figure 4) for  $\sigma_2 = 41.2201$ ,  $\mu=0.1$ ,  $\alpha=0$ ,  $v_1=10$  and  $\sigma_1 = 44.00$

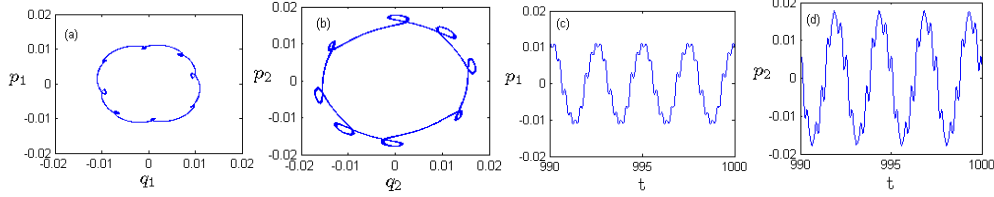


Figure 6: Phase portraits (a, b) and time traces (c, d) for  $\sigma_2 = 74.5201$ ,  $\mu=0.1$ ,  $\alpha=0$ ,  $v_1=10$  and  $\sigma_1 = 44.00$

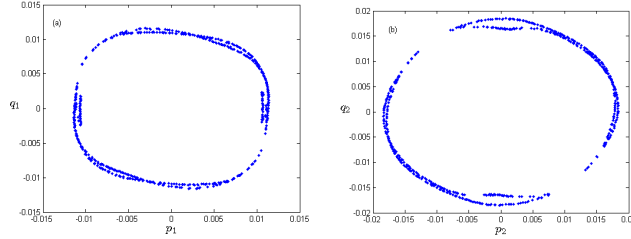


Figure 7: Poincare maps (a, b) for  $\sigma_2 = 82.5201$ ,  $\mu=0.1$ ,  $\alpha=0$ ,  $v_1=10$  and  $\sigma_1 = 44.00$

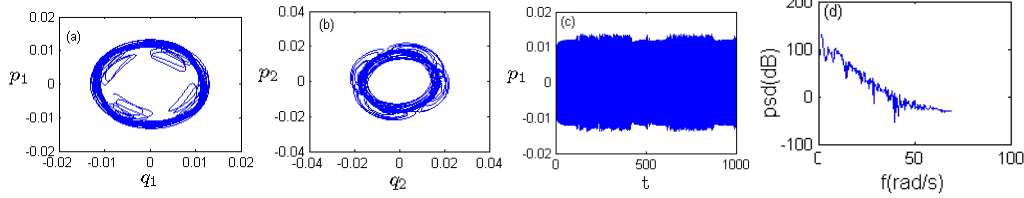


Figure 8: Phase portraits (a, b), time history (c) and FFT power spectra (d) for  $\sigma_2 = 85.5201$ ,  $\mu=0.1$ ,  $\alpha=0$ ,  $v_1=10$  and  $\sigma_1 = 44.00$

## 5 CONCLUSIONS

For travelling beam, the influence of internal resonance is demonstrated by two mode equilibrium solutions of amplitude and frequency response analysis. The isolated closed loop two mode solutions are found to be fixed between two limit points for specific ranges of control parameters because of the nonlinear modal interaction due to three to one internal resonance. The amplitude of other nontrivial solution for first mode increases monotonically with no upper bound when  $\sigma_2$  increases while for second mode, it decreases to a lower fixed value. The strength of nonlinear modal interactions increases for higher values of harmonic component of travelling velocity. It is observed that a lower value of frequency detuning parameter weakens the modal interaction due to 3:1 internal resonance and it is more pronounced in first mode compared to that of the second mode. The system exhibits saddle node and Hopf bifurcations for variation in control parameters.

The dynamic solutions in the form of periodic, quasi-periodic and chaotic are captured with the help of time history, phase portraits and Poincare maps. The system exhibits jump phenomena due to variations of control parameters. The system behavior changes to chaotic



response through quasi periodic route. With variation of control parameter, the system experiences an array of dynamic responses.

## REFERENCES

- [1] J.A. Wickert, C.D. Mote Jr., Current research on the vibration and stability of axially moving materials. *Shock and Vibration Digest*, 20, 3-13, 1988.
- [2] J.A. Wickert, C.D. Mote Jr., Classical vibration analysis of axially moving continua, *Journal of Applied Mechanics*, 57, 738-744, 1990.
- [3] J.A. Wickert, C.D. Mote Jr., Traveling load response of an axially moving string, *Journal of Sound and Vibration*, 149, 267-248, 1991.
- [4] H.R. Oz, M.Pakdemirli, Vibrations of an axially moving beam with time-dependent velocity, *Journal of Sound and Vibration*, 227(2), 239-257, 1999.
- [5] H.R. Oz, M.Pakdemirli, H.Boyaci, Non-linear Vibrations of an axially moving beam with time-dependent velocity, *International Journal of Non-linear Mechanics*, 36, 227(2), 107-115, 2001.
- [6] C.H.Riedel, C.A. Tan, Coupled, forced response of an axially moving strip with internal resonance, *International Journal of Nonlinear Mechanics*, 37, 101-116.
- [7] E.Ozkaya, S.M.Bagdatli, H.R. Oz, Nonlinear transverse vibrations and 3:1 internal resonances of a beam with multiple supports, *Journal of Vibration and Acoustics*, 130(2), 1-11, 2008
- [8] C.M. Chin, A.H. Nayfeh, Three-to-one internal resonance in parametrically excited Hinged-clamped beams, *Nonlinear Dynamics*, 20, 131-158, 1999.
- [9] L.N. Panda, R.C. Kar, Nonlinear dynamics of a pipe conveying pulsating fluid with parametric and internal resonances, *Nonlinear Dynamics*, 49, 9-30, 2007.
- [10] L.N. Panda, R.C. Kar, Nonlinear dynamics of a pipe conveying pulsating fluid with combination, principal parametric and internal resonances, *Journal of Sound and Vibration*, 309, 375-406, 2008.
- [11] H. Ding and L.-Q. Chen, Galerkin methods for natural frequencies of high-speed axially moving beams, *Journal of Sound and Vibration*, 329, 3484-3494, 2010.
- [12] M. Pakdemirli and H.R. Oz, Infinite mode analysis and truncation to resonant modes of axially accelerated beam vibrations, *Journal of Sound and Vibration*, 311, 1052-1074, 2008.
- [13] S.V. Ponomareva and W.T. van Horssen, On the transversal vibration of an axially moving continuum with a time-varying velocity: Transient from string to beam behavior, *Journal of Sound and Vibration*, 325, 959-973, 2009.
- [14] M.H. Ghayesh, Nonlinear forced dynamics of an axially moving viscoelastic beam with an internal resonance, *International Journal of Mechanical Sciences*, 53, 1022-1037, 2011.
- [15] M.H. Ghayesh, H.A. Kafiabad and T. Reid, Sub and super critical nonlinear dynamics of a harmonically excited axially moving beam, *International Journal of Solids and Structures*, 49, 227-243, 2012.

- [16] G. Chakraborty and A.K. Mallick, Stability of an accelerating beam, *Journal of Sound and Vibration*, 27(2), 309-320, 1999
- [17] M.P. Paidoussis, Flutter of conservative systems of pipe conveying incompressible fluid, *Journal of Mechanical Engineering and Science*, 17(1), 1975

## APPENDIX

$$\Gamma_1 = -2i\omega_1 A_1' \phi_1 - 2v_0 A_1' \phi_1' - 2i\mu\omega_1 A_1 \phi_1 - 2i\alpha\omega_1 A_1 \phi_1'''' \frac{1}{2} v_i^2 \left\{ 2A_1^2 \bar{A}_1 \phi_1' \int_0^1 \phi_1' \bar{\phi}_1 dx + A_1^2 \bar{A}_1 \phi_1'' \int_0^1 \phi_1^2 dx + 2A_1 A_2 \bar{A}_2 \phi_2' \int_0^1 \phi_1' \phi_2' dx \right. \\ \left. + 2A_1 A_2 \bar{A}_2 \phi_1' \int_0^1 \phi_2' \bar{\phi}_2 dx + 2A_1 A_2 \bar{A}_2 \phi_1'' \int_0^1 \phi_2' \bar{\phi}_2 dx \right\} \quad (A1) \quad \Gamma_2 = \frac{1}{2} v_i^2 \left\{ 2\bar{A}_1^2 A_2 \bar{\phi}_1' \int_0^1 \phi_2' \bar{\phi}_1 dx + \bar{A}_1^2 A_2 \phi_2' \int_0^1 \bar{\phi}_1^2 dx \right\} \quad (A2)$$

$$\Gamma_3 = \bar{A}_1 \left\{ v_1 \omega_1 \bar{\phi}_1' - \frac{v_1 \Omega}{2} \bar{\phi}_1 + i v_0 v_1 \bar{\phi}_1'' \right\} \quad (A3)$$

$$\Gamma_5 = -2i\omega_2 A_2' \phi_2 - 2v_0 A_2' \phi_2' - 2i\mu\omega_2 A_2 \phi_2 - 2i\alpha\omega_2 A_2 \phi_2'''' \frac{1}{2} v_i^2 \left\{ A_2^2 \bar{A}_2 \phi_2' \int_0^1 \phi_2^2 dx + 2A_1 \bar{A}_1 A_2 \phi_2' \int_0^1 \phi_1' \bar{\phi}_1 dx + 2A_1 \bar{A}_1 A_2 \phi_2'' \int_0^1 \phi_1' \phi_2' dx \right. \\ \left. + 2A_1^2 \bar{A}_2 \phi_2' \int_0^1 \phi_2' \bar{\phi}_2 dx + 2A_1 \bar{A}_1 A_2 \phi_1' \int_0^1 \phi_2' \bar{\phi}_1 dx \right\} \quad (A4) \quad \Gamma_6 = \frac{1}{2} v_i^2 \left\{ A_1^3 \phi_1' \int_0^1 \phi_1^2 dx \right\} \quad (A5) \quad \Gamma_8 = \bar{A}_2 \left\{ v_1 \omega_2 \bar{\phi}_2' - \frac{v_1 \Omega}{2} \bar{\phi}_2 + i v_0 v_1 \bar{\phi}_2'' \right\} \quad (A6)$$

$$S_1 = \frac{\frac{1}{16} v_i^2 \left\{ 2 \int_0^1 \phi_1' \bar{\phi}_1 dx \int_0^1 \phi_1' \bar{\phi}_1 dx + \int_0^1 \phi_1' \bar{\phi}_1 dx \int_0^1 \phi_1^2 dx \right\}}{-\left\{ i\omega_1 \int_0^1 \phi_1 \bar{\phi}_1 dx + v_0 \int_0^1 \phi_1' \bar{\phi}_1 dx \right\}} \quad (A7) \quad S_2 = \frac{\frac{1}{8} v_i^2 \left\{ \int_0^1 \phi_2' \bar{\phi}_2 dx \int_0^1 \phi_1' \phi_2' dx + \int_0^1 \phi_1' \bar{\phi}_1 dx \int_0^1 \phi_2' \bar{\phi}_2 dx + \int_0^1 \phi_1' \bar{\phi}_1 dx \int_0^1 \phi_2' \bar{\phi}_2 dx \right\}}{-\left\{ i\omega_1 \int_0^1 \phi_1 \bar{\phi}_1 dx + v_0 \int_0^1 \phi_1' \bar{\phi}_1 dx \right\}} \quad (A8)$$

$$S_3 = \frac{\frac{1}{8} v_i^2 \left\{ \int_0^1 \phi_2' \bar{\phi}_2 dx \int_0^1 \phi_1' \bar{\phi}_1 dx + \int_0^1 \phi_1' \bar{\phi}_1 dx \int_0^1 \phi_2' \bar{\phi}_2 dx + \int_0^1 \phi_1' \bar{\phi}_1 dx \int_0^1 \phi_2' \bar{\phi}_2 dx \right\}}{-\left\{ i\omega_2 \int_0^1 \phi_2 \bar{\phi}_2 dx + v_0 \int_0^1 \phi_2' \bar{\phi}_2 dx \right\}} \quad (A9) \quad S_4 = \frac{\frac{1}{16} v_i^2 \left\{ 2 \int_0^1 \phi_2' \bar{\phi}_2 dx \int_0^1 \phi_2' \bar{\phi}_2 dx + \int_0^1 \phi_2' \bar{\phi}_2 dx \int_0^1 \phi_2^2 dx \right\}}{-\left\{ i\omega_2 \int_0^1 \phi_2 \bar{\phi}_2 dx + v_0 \int_0^1 \phi_2' \bar{\phi}_2 dx \right\}} \quad (A10)$$

$$C_1 = \frac{-i\omega_1 \int_0^1 \phi_1 \bar{\phi}_1 dx}{-\left\{ i\omega_1 \int_0^1 \phi_1 \bar{\phi}_1 dx + v_0 \int_0^1 \phi_1' \bar{\phi}_1 dx \right\}} \quad (A11) \quad C_2 = \frac{-i\omega_2 \int_0^1 \phi_2 \bar{\phi}_2 dx}{-\left\{ i\omega_2 \int_0^1 \phi_2 \bar{\phi}_2 dx + v_0 \int_0^1 \phi_2' \bar{\phi}_2 dx \right\}} \quad (A12) \quad e_1 = \frac{-i\omega_1 \int_0^1 \phi_1'''' \bar{\phi}_1 dx}{-\left\{ i\omega_1 \int_0^1 \phi_1 \bar{\phi}_1 dx + v_0 \int_0^1 \phi_1' \bar{\phi}_1 dx \right\}} \quad (A13)$$

$$e_2 = \frac{-i\omega_2 \int_0^1 \phi_2'''' \bar{\phi}_2 dx}{-\left\{ i\omega_2 \int_0^1 \phi_2 \bar{\phi}_2 dx + v_0 \int_0^1 \phi_2' \bar{\phi}_2 dx \right\}} \quad (A14) \quad g_1 = \frac{\frac{1}{16} v_i^2 \left\{ 2 \int_0^1 \phi_1' \bar{\phi}_1 dx \int_0^1 \phi_2' \bar{\phi}_1 dx + \int_0^1 \phi_2' \bar{\phi}_1 dx \int_0^1 \bar{\phi}_1^2 dx \right\}}{-\left\{ i\omega_1 \int_0^1 \phi_1 \bar{\phi}_1 dx + v_0 \int_0^1 \phi_1' \bar{\phi}_1 dx \right\}} \quad (A15) \quad g_2 = \frac{\frac{1}{16} v_i^2 \left\{ \int_0^1 \phi_1' \bar{\phi}_1 dx \int_0^1 \phi_1^2 dx \right\}}{-\left\{ i\omega_2 \int_0^1 \phi_2 \bar{\phi}_2 dx + v_0 \int_0^1 \phi_2' \bar{\phi}_2 dx \right\}} \quad (A16)$$

$$K_4 = \frac{\frac{1}{2} \left\{ v_1 \omega_2 \int_0^1 \phi_2' \bar{\phi}_1 dx - \frac{v_1 \Omega}{2} \int_0^1 \phi_2' \bar{\phi}_1 dx + i v_0 v_1 \int_0^1 \phi_2'' \bar{\phi}_1 dx \right\}}{-\left\{ i\omega_1 \int_0^1 \phi_1 \bar{\phi}_1 dx + v_0 \int_0^1 \phi_1' \bar{\phi}_1 dx \right\}} \quad (A17) \quad K_5 = \frac{\frac{1}{2} \left\{ v_1 \omega_1 \int_0^1 \phi_1' \bar{\phi}_2 dx - \frac{v_1 \Omega}{2} \int_0^1 \phi_1' \bar{\phi}_2 dx + i v_0 v_1 \int_0^1 \phi_1'' \bar{\phi}_2 dx \right\}}{-\left\{ i\omega_2 \int_0^1 \phi_2 \bar{\phi}_2 dx + v_0 \int_0^1 \phi_2' \bar{\phi}_2 dx \right\}} \quad (A18)$$